LİBYA'DA GÜNEŞ ENERJİLİ ABSORPSİYON SİSTEMLERİ İLE SICAK İKLİMLERDE SÜRDÜRÜLEBİLİR SOĞUTMA

Abdulrazzak AKROOT [1]/ Jamal Basheer ALBARTOULI [2]
[1] Karabük Üniversitesi, Mühendislik Fakültesi Makine Mühendisliği Bölümü, Karabük-Türkiye
abdulrazzakakroot@karabuk.edu.tr ORCID: 0000-0002-1561-7260
[2] Karabük Üniversitesi, Mühendislik Fakültesi Makine Mühendisliği Bölümü, Karabük-Türkiye
ORCID: 0009-0006-8648-5820

Özet

Sıcak ve kurak bölgelerde artan küresel soğutma talebi, enerji güvenliği, çevresel sürdürülebilirlik ve ekonomik kalkınma açısından kritik zorluklar ortaya koymaktadır. Bol güneş enerjisi kaynaklarına sahip olmasına rağmen geleneksel elektrikle çalışan klima sistemlerine yoğun bağımlılığı olan Libya, yenilenebilir enerjiye dayalı çözümleri araştırmak için ideal bir ortam sunmaktadır. Bu çalışma, Libya'nın üç büyük şehrinin (Trablus, Bingazi ve Misrata) iklim koşullarına uygun olarak tasarlanan güneş destekli absorpsiyonlu soğutma sisteminin fizibilitesini ve performansını değerlendirmektedir. Farklı işletim ve çevresel parametreler altında sistem performansını incelemek için enerji ve ekserji analizleri yapılmıştır. Sonuçlar, toplam ekserji yıkımının yaklaşık %80'inden sorumlu olan parabolik oluk toplayıcının (PTC) başlıca verimsizlik kaynağı olduğunu, buna karşın jeneratör ve çözelti ısı değiştirici gibi bileşenlerin daha yüksek verimlilik sergilediğini göstermektedir. Doğrudan normal ışınım (DNI) ve soğutma yükündeki mevsimsel değişimler incelenmiş, özellikle Bingazi'de yaz aylarında soğutma talebinin en yüksek düzeylere ulaştığı ve güneş enerjisi potansiyelinin maksimum seviyelere çıktığı görülmüştür. Sistem, yaklaşık 0.75–0.8 arasında sabit bir performans katsayısı (COP) ve 0.35 civarında ekserji verimliliği elde etmiş, yaz aylarında soğutma yükü 10 kW'ın üzerine çıkmıştır. Bulgular, güneş destekli absorpsiyonlu soğutma sistemlerinin Libya'da geleneksel klima sistemlerine sürdürülebilir ve güvenilir bir alternatif sağlayabileceğini ve performansın iklimsel farklılıklara bağlı olarak değiştiğini doğrulamaktadır.

Anahtar Kelimeler: Güneş enerjisi, Absorpsiyonlu soğutma, Ekserji analizi, Sürdürülebilir soğutma, Libya iklim koşulları,

SUSTAINABLE COOLING IN HOT CLIMATES THROUGH SOLAR ABSORPTION SYSTEMS IN LIBYA

Abdulrazzak AKROOT [1]/ Jamal Basheer ALBARTOULI [2]
[1] Karabük University, Faculty of Engineering Department of Mechanical Engineering, Karabük-Türkiye
abdulrazzakakroot@karabuk.edu.tr ORCID: 0000-0002-1561-7260
[2] Karabük University, Faculty of Engineering Department of Mechanical Engineering, Karabük-Türkiye
ORCID: 0009-0006-8648-5820

Abstract

The rising global demand for cooling in hot and arid regions poses critical challenges for energy security, environmental sustainability, and economic development. Libya, with its abundant solar resources yet heavy dependence on conventional electricity-driven air conditioning, represents an ideal setting to investigate renewable-based solutions. This study evaluates the feasibility and performance of a solar-assisted absorption cooling system designed for the climatic conditions of three major Libyan cities: Tripoli, Benghazi, and Misrata. Energy and exergy analyses were conducted to assess system performance under varying operational and environmental parameters. Results highlight that the parabolic trough collector is the major source of exergy destruction, accounting for nearly 80% of irreversibility, while components such as the generator and solution heat exchanger demonstrate higher efficiencies. Seasonal variations in direct normal irradiance (DNI) and cooling load were analyzed, showing peak cooling demand and maximum solar potential during summer months, particularly in Benghazi. The system achieved a stable coefficient of performance (COP) of around 0.75–0.8 and exergy efficiency of approximately 0.35 across operating conditions, with the cooling load exceeding 10 kW during peak summer. The findings confirm that solar-assisted absorption cooling systems can provide a sustainable and reliable alternative to conventional air conditioning in Libya, with performance varying by location due to climatic differences.

Keywords: Solar energy, Absorption cooling, Exergy analysis, Sustainable cooling, Libyan climate conditions

1- INTRODUCTION

Global climate change, rapid urbanization, and the intensification of heat waves have created unprecedented growth in global cooling demand (Birol, 2018; Sivak, 2009). This issue is particularly acute in hot and arid regions such as North Africa and the Middle East, where cooling is not a luxury but a fundamental requirement for health, productivity, and economic stability (Schilling et al., 2020). In Libya, soaring summer temperatures and population growth have driven electricity consumption for air conditioning to record levels, placing immense strain on an already fragile electricity grid (Bindra SP, Soul F, Jabu SD, Allawafi A, Belashher AM, 2015). The key challenge is how to meet this growing demand for cooling while reducing dependence on fossil fuels, lowering greenhouse gas emissions, and ensuring long-term sustainability. Solar-assisted absorption cooling systems have emerged as a promising alternative to address these interrelated challenges (Akroot et al., 2024; Oye et al., 2020).

Several previous studies have highlighted the technical and economic potential of solar cooling. Suwaed et al., (2023) demonstrated that improving solar collector designs could increase efficiency by up to 20%, making solar cooling more feasible in arid regions. Similarly, Bakry et al., (2025) analyzed solar absorption systems in Egypt, finding that the most significant advantage was the reduction in electricity consumption, which alleviates stress on national grids. (Bakhshi-Jafarabadi & Seyed Mousavi, 2024) investigated a rooftop photovoltaic system installed on a commercial building in an arid region and found that it shaved 12–18 % of peak air-conditioning demand at midday, all without relying on battery storage.

Other researchers have focused on seasonal and technical performance. Al-Falahi et al., (2020) conducted a TRNSYS-based case study in Baghdad (a hot climate similar to Libya's), finding that the system achieved its highest average COP (0.52), and solar fraction (59.4 %)in August, demonstrating that seasonal conditions, particularly peak summer solar potential, can significantly enhance performance. Ibrahim et al., (2020) conducted an extensive parametric analysis under varied solar conditions, demonstrating that a solar-driven double-effect absorption chiller delivers notably higher energy and exergy performance than a single-effect system, confirming the enhanced efficiency of multi-effect configurations when paired with solar thermal sources. A recent report from the Global Cooling Watch Tryndina et al., (2022) underscores that around 66% of global cooling-related emissions currently come from developing countries, and that the transition to sustainable cooling, including solar cooling, depends heavily on improved regulations, enforcement, and especially access to finance

Regionally, Imghoure et al., (2024) investigated passive cooling strategies by enhancing wall materials in Moroccan residential buildings under semi-arid conditions. Their simulations showed a striking 52 % reduction in summer energy use, resulting in a 39 % reduction in associated CO_2 emissions, highlighting the environmental impact of integrating advanced building envelope design. In a recent MENA-wide modeling assessment, Hasanain, (2024) showed that solar-assisted absorption cooling systems can achieve a payback period as short as 5.8 years, offering a compelling case for their economic competitiveness in hot climates. In terms of modeling, Hu et al., (2022) developed a comprehensive predictive framework by integrating steady-state models of a solar-driven absorption chiller and a radiative sky cooling system with load simulations, enabling a promising strategy for 24-hour continuous cooling performance optimization. In Tunisia, Balghouthi et al., (2012) documented a solar cooling installation that harnessed parabolic trough collectors and a double-effect absorption chiller, achieving system COPs ranging from 0.65 to 1.29 and daily solar COPs up to 0.35, demonstrating early.

Together, these studies clearly underscore the potential of solar-assisted cooling technologies. However, very few have directly addressed Libya's unique conditions. With direct normal irradiance (DNI) exceeding 7.5 kWh/m² per day in many locations, Libya has one of the world's richest solar resources (Bodalal et al., 2017). Yet, regional variations in temperature, humidity, and seasonal solar availability across cities such as Tripoli, Benghazi, and Misrata complicate system performance generalizations (Ali, 2025; Elsharkawy & Elmallah, 2016). Benghazi,

for example, records some of the highest DNI values during summer, making it an ideal candidate for solar cooling, whereas Misrata may face challenges due to lower irradiation and humidity constraints. This diversity highlights the need for localized assessments that adapt system design to specific climatic conditions (Bakouri et al., 2023; Gnedi & Robaa, 2024).

Beyond energy considerations, the sustainability dimension of cooling is gaining traction globally. Solar-assisted absorption cooling aligns with international frameworks such as the Paris Agreement and the United Nations Sustainable Development Goals by reducing fossil fuel dependence and curbing emissions (SECRETARIAT, 2002; Weltbankgruppe, 2021). Techno-economic assessments suggest that when optimized for local climatic conditions, solar-assisted cooling systems can achieve competitive payback periods—in one study examining sun-belt cities in Saudi Arabia, a 50 kW system achieved a payback period of approximately 9.9 years using evacuated tube collectors (Hasan & Mokheimer, 2024).

For Libya, adopting solar-assisted absorption cooling not only addresses energy and environmental concerns but also offers economic opportunities in transitioning toward a more resilient and sustainable energy future. For instance: A recent techno-economic study highlights that solar-assisted absorption systems, when paired with double-effect configurations and optimized solar collectors, can outperform conventional setups, achieving lower operational costs (approximately $5.2/hour) and competitive levelized costs (approx. $0.14/GJ) under sunbelt conditions (Al-Falahi et al., 2021).

The originality of this research lies in its comprehensive and comparative assessment of solar-assisted absorption cooling systems under Libya's diverse climatic conditions, using integrated energy and exergy analyses. Unlike most previous studies, which have focused on generalized performance or on other countries, this study systematically compares three major Libyan cities, Tripoli, Benghazi, and Misrata, demonstrating how local variations in solar radiation, temperature, and cooling demand affect system outcomes. By combining rigorous thermodynamic modeling with location-specific data, the study fills a critical knowledge gap and provides actionable insights for policymakers, engineers, and investors. Its distinctive contribution lies in showing that solar absorption cooling can move beyond being a pilot technology to become a scalable, sustainable solution for countries grappling with rapidly rising cooling demands in hot climates.

2. SYSTEM DESCRIPTINS

Figure 1 illustrates a single-effect LiBr–H_2O absorption chiller powered by solar parabolic trough collectors. Solar heat is used to drive the generator, where water vapor acts as the refrigerant. The cycle consisting of generator, condenser, evaporator, and absorber, delivers cooling for buildings, with pumps, valves, and a solution heat exchanger. On the left, the Solar parabolic trough collector (PTC) Field is used to capture solar radiation and convert it into thermal energy. A working fluid (often a heat transfer fluid such as thermal oil or pressurized water) circulates through the collector tubes. This hot fluid is pumped by pump 1 into a thermal storage tank , which acts as a buffer to store thermal energy for continuous operation. The Thermal Storage Tank ensures stability by balancing fluctuations in solar radiation. Pump 2 circulates the hot fluid (position 4) from the tank into the generator. The generator receives the heat from the thermal storage. Here, a LiBr–H_2O solution is separated. Water vapor (refrigerant) is boiled off (stream 13), The concentrated LiBr solution (stream 9) is sent to the solution heat exchanger (SHEX). The SHEX improves efficiency by preheating the weak LiBr solution (from the absorber) before it enters the generator. The water vapor from the generator moves to the condenser (stream 13 → 17). In the condenser, heat is rejected to the environment, and the vapor condenses into liquid water refrigerant. The liquid refrigerant is throttled through expansion valve1(stream 14 → 15), lowering its pressure and temperature. It then enters the evaporator (stream 15 → 21), where it absorbs heat from the building's cooling load, producing chilled water or air. This process provides the actual cooling effect delivered to the building (stream 22). The low-pressure water vapor leaving the evaporator (stream 21) is absorbed into the

concentrated LiBr solution in the Absorber. This absorption process releases heat, which must be rejected (stream 19). Cooling water is used to maintain absorber efficiency. The weak solution from the absorber is pumped (via Pump 3) through the SHEX (stream 7 → 8) and back into the generator (stream 9), closing the cycle.

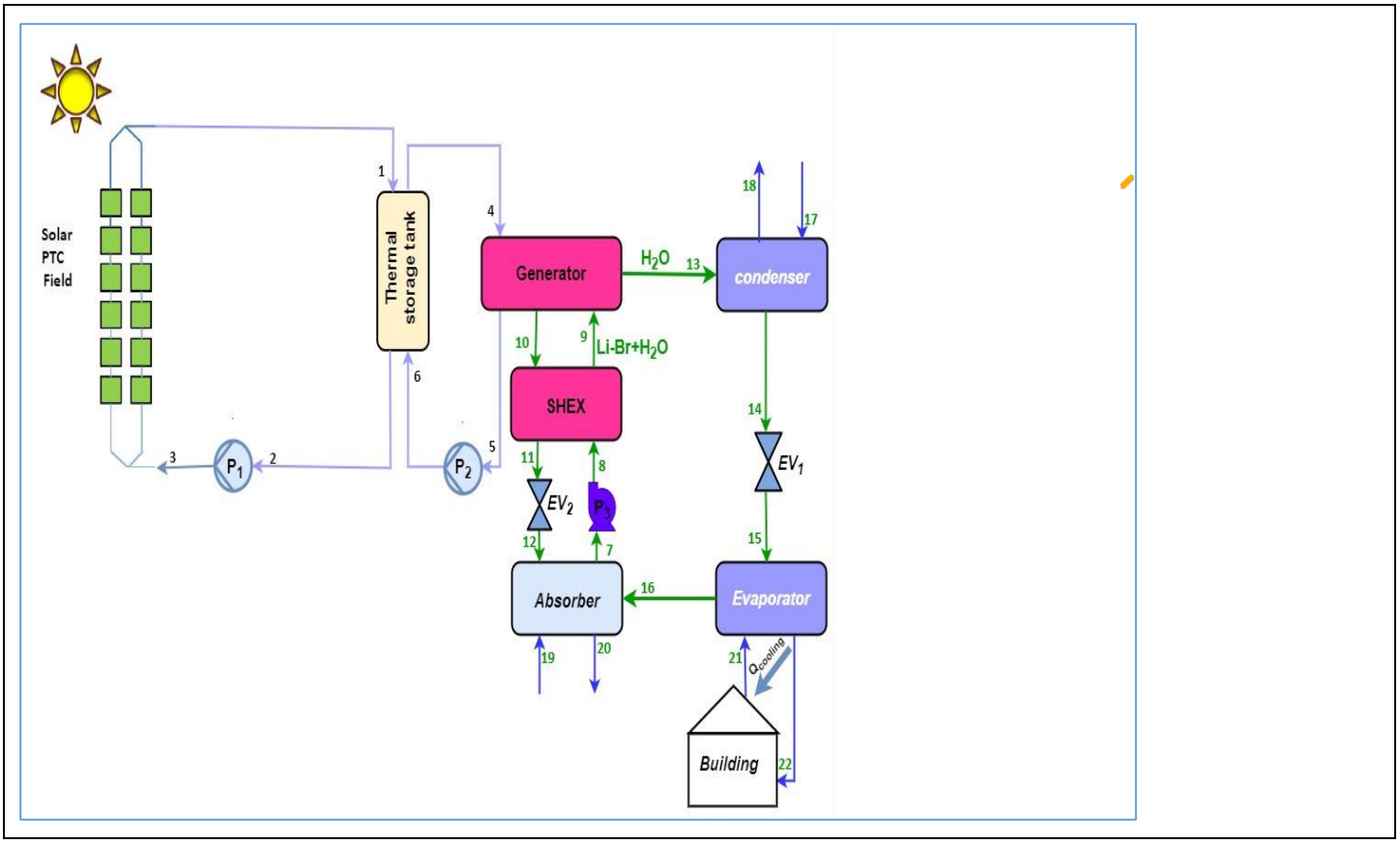

Figure1: Schematic Diagram of a Solar Absorption Cooling System for Libyan Cities (Tripoli, Benghazi, and Misrata)

In Benghazi, the consistently high levels of direct normal irradiance (DNI) during summer make the solar-assisted cooling system particularly effective, with the solar field capable of supplying the majority of the thermal demand. In contrast, Misrata experiences relatively lower DNI combined with higher humidity, conditions that may necessitate either larger thermal storage capacity or auxiliary backup to ensure stable operation. Meanwhile, Tripoli presents a more balanced scenario, where moderate solar availability and cooling demand result in intermediate system performance.

Table 3.1 presents the input data for modeling the proposed solar absorption cooling system. The system modeling is carried out based on the following assumptions:

1. Each component of the system is assumed to operate under steady-state conditions.
2. Pressure drops in piping and the heat exchanger are negligible due to their minimal effect, except for the notable pressure drops across the expansion valves between points 11 and 12 and 14 and 15 (refer to FigURE1).
3. The working fluid is assumed to exit the condenser as a saturated liquid and the evaporator as a saturated vapor.

4. The work input by the circulating pump is disregarded, as it is insignificant compared to the thermal energy supplied to the generator.
5. Exergy calculations are based on the specific enthalpy and entropy values of water at standard environmental conditions (25 °C and 1 atm).
6. Kinetic and potential energy and exergy contributions are ignored due to their relatively minor influence on the system.

Table 1: Input data for modeling of the suggested system.

Parameter	**Value**
Solar area (m^2)	71.16 m2
Sun temperature	5770 K
DNI	7.92 kWh/ m2.day
PTC outlet temperature	243° C
PTC inlet temperature	120.1° C
Tamb	25° C
Pamb	101kPa
Absorber temperature (T_7)	33° C
Generator temperature (T_{10})	81.39° C
LiBr solution strength	54.3%
Pumps efficiency	80%
Solution heat exchanger effectiveness	57%

The fundamental concepts of continuity and the first law of thermodynamics are summarized below (Dawahdeh & Al-Nimr, 2025; Talal & Akroot, 2024):

$$\sum_{in} \dot{m}_{in} = \sum_{out} \dot{m}_{out} \quad (1)$$

$$\sum_{in} \dot{m}_{in}\, x_{in} = \sum_{out} \dot{m}_{out}\, x_{out} \quad (2)$$

where $\dot{m}_{in}$ is the entered mass flow rate, $\dot{m}_{out}$ is the exit mass flow rate, x_{in} is the LiBr concentration at the inlet and x_{out} is the LiBr concentration at the outlet.

The following equation allows us to model energy interactions in steady-state processes. It ensures a comprehensive energy analysis and highlights efficiency and losses in the system (Lu et al., 2020; Talal & Akroot, 2023):

$$\dot{Q}_{in} + \dot{W}_{in} + \sum_{in} \dot{m}(h_{in}) = \dot{Q}_{out} + \dot{W}_{out} + \sum_{out} \dot{m}(h_{out}) \quad (3)$$

Where: "$\dot{W}$" refers to the work produced, "$\dot{m}$" refers to the mass flow rate,"$\dot{Q}$" refers to the heat input, and "h" refers to the enthalpy. The letters 'in' and 'out' in the subscript denote the inlet and output states.

The exergy rate is the most useful theoretical work achieved when a system transforms from its initial state to thermal and mechanical equilibrium with its surroundings. The following formula for exergy balance will be used to determine each part's exergy destruction (Elmorsy et al., 2020):

$$\dot{E}_Q - \dot{E}_W = \sum \dot{E}_{out} - \sum \dot{E}_{in} - \dot{E}_{Dest} \quad (4)$$

Where: " $\dot{E}_Q$" refers to the exergy rate for heat transfer (MW)," $\dot{E}_W$" represents the exergy rate for work transfer (MW)," $\dot{E}_{out}$" indicates the exergy rate for system outputs (MW), " $\dot{E}_{in}$" refers to the exergy rate for system inputs (MW), and" $\dot{E}_{Dest}$" refers to the exergy destruction rate (MW). The stream exergy rate by heat is determined using the following equation (Akroot, 2025; Wang et al., 2019).

$$\dot{E}_Q = \left(1 - \frac{T_{amb}}{T_i}\right) \dot{Q}_i \quad (5)$$

Where: "T_{amb}", indicates the environment temperature for a dead state (K),"T_i" refers to the system boundary temperature for heat transfer happens (K), and"$\dot{Q}_i$", represents the heat transfer rate (MW). The exergy balance for a system in a steady state is stated as follows:

$$\dot{E}_f = \dot{E}_p + \dot{E}_{dest} \quad (6)$$

Here, $\dot{E}_f$, $\dot{E}_p$, and $\dot{E}_{dest}$ represent the exergy flow of fuel, product, and destruction, respectively. According to the second law analysis, the exergy destruction rate represents the loss of the ability to convert energy into usable work. To examine a system's exergy efficiency, the fuel and product exergy of each component are evaluated using the surplus efficiency principles (Nourpour et al., 2023):

$$\eta_{ex} = \left(1 - \frac{\dot{E}_{dest}}{\dot{E}f}\right) = \frac{\dot{E}p}{\dot{E}f} \quad (7)$$

where η_{ex}represents the exergy efficiency. The coefficient performance of the absorption system (COP) is given as (Akroot & Refaei, 2025):

$$COP = \frac{\dot{Q}_{Evap}}{\dot{Q}_{Gen}} \quad (8)$$

The energetic efficiency of the system is assessed using the system coefficient of performance (SCOP), which is defined as follows:

$$SCOP = \frac{\dot{Q}_{Evap}}{\dot{Q}_{Solar}} \quad (9)$$

The system exergy efficiency (η_{ex}) is defined as:

$$\eta_{ex} = \frac{\dot{Q}_{\text{Evap}} \cdot \left(\frac{T_0}{T_e} - 1\right)}{\dot{Q}_{\text{Solar}} \cdot \left[1 - \frac{4}{3} \cdot \frac{T_0}{T_{\text{sun}}} + \frac{1}{3} \cdot \left(\frac{T_0}{T_{\text{sun}}}\right)^4\right]} \quad (10)$$

Table 1. Energy and Exergy balance equations for all components of the Model 3 system**.**

Component	Energy Balances	Exergy Balances
PTC	$\dot{Q}_{solar} = \eta_{PTC} * A_{ap} * DNI$	$\dot{E}_{Q,solar} = \left(1 - \frac{T_0}{T_{sun}}\right) \dot{Q}_{solar}$
TST	$\dot{Q}_{TST} = \dot{m}_1(h_1 + h_2)$	$\dot{E}_{D,TST} = \dot{E}_1 + \dot{E}_6 - \dot{E}_4 - \dot{E}_2$
Pump$_1$	$\dot{W}_{Pump_1} = \dot{m}_2(h_3 - h_2)$	$\dot{E}_{D,Pump_1} = \dot{W}_{Pump_1} + \dot{E}_2 - \dot{E}_3$
Pump$_2$	$\dot{W}_{Pump_2} = \dot{m}_5(h_6 - h_5)$	$\dot{E}_{D,Pump_2} = \dot{W}_{Pump_2} + \dot{E}_5 - \dot{E}_6$
Gen	$\dot{Q}_{Gen} = \dot{m}_4(h_4 - h_5)$	$\dot{E}_{D,Gen} = \dot{E}_4 + \dot{E}_9 - \dot{E}_5 - \dot{E}_{10} - \dot{E}_{11}$
Abs	$\dot{Q}_{Abs} = \dot{m}_7 h_7 - \dot{m}_{16} h_{16} - \dot{m}_{12} h_{12}$	$\dot{E}_{D,Abs} = \dot{E}_{12} + \dot{E}_{16} - \dot{E}_7 + \dot{E}_{19} - \dot{E}_{20}$
SHEX	$\dot{Q}_{SHEX} = \dot{m}_{10}(h_{10} - h_{11})$	$\dot{E}_{D,SHEX} = \dot{E}_{10} + \dot{E}_8 - \dot{E}_9 - \dot{E}_{11}$
Pump$_3$	$\dot{W}_{Pump_3} = \dot{m}_7(h_8 - h_7)$	$\dot{E}_{D,Pump_3} = \dot{W}_{Pump_3} + \dot{E}_7 - \dot{E}_8$
Evap	$\dot{Q}_{Evap} = \dot{m}_{15}(h_{16} - h_{15})$	$\dot{E}_{D,\,Evap} = \dot{E}_{15} + \dot{E}_{22} - \dot{E}_{16} - \dot{E}_{21}$
Ev$_1$	$\dot{m}_{14} h_{14} = \dot{m}_{15} h_{15}$	$\dot{E}_{D,Ev_1} = \dot{E}_{15} - \dot{E}_{16}$
Ev$_2$	$\dot{m}_{11} h_{11} = \dot{m}_{12} h_{12}$	$\dot{E}_{D,Ev_2} = \dot{E}_{11} - \dot{E}_{12}$
Cond	$\dot{Q}_{con} = \dot{m}_{13}(h_{13} - h_{14})$	$\dot{E}_{D,Cond} = \dot{E}_{13} - \dot{E}_{14} + \dot{E}_{17} - \dot{E}_{18}$

3. RESULTS AND DİSCUSSİONS

Table 3 presents a detailed exergy analysis for each major solar-assisted absorption cooling system component. The table includes three key performance metrics: exergy destruction (kW), percentage of total exergy destruction (%), and exergy efficiency (%). The table highlights that the parabolic trough collector (PTC) is the main source of exergy destruction, drastically affecting overall system efficiency. On the other hand, components like EV$_2$, TST, Generator, and SHEX demonstrate high exergy efficiency, indicating strong performance in their respective roles. The PTC is the dominant source of irreversibility, accounting for nearly 80% of total exergy destruction, primarily due to large temperature gradients between the solar source and the working fluid. TST has relatively low exergy destruction and high efficiency, suggesting good insulation and thermal management in the storage system. The generator shows high exergy efficiency, indicating that it performs well in utilizing the input thermal energy from the collector. Its moderate exergy destruction reflects conversion losses but remains one of the better-performing units. The condenser suffers from significant irreversibility and low exergy efficiency, likely due to heat rejection to the environment. Enhancing heat recovery or lowering temperature differentials could improve its performance. The absorber shows moderate inefficiency, likely due to mass and heat transfer limitations between the refrigerant and absorbent. There's room for improving absorber design or heat exchanger surface area. The SHEX performs well, contributing minimally to exergy loss while improving internal heat recovery and overall system thermal economy. With moderate exergy destruction and reasonable efficiency, the evaporator plays a stable role in the cooling cycle, though improvements in temperature match between working fluid and surroundings may help.

Table 3: Exergy analysis for each solar-assisted absorption cooling system component.

Component	Exergy destruction (kW)	Exergy destruction Percentage (%)	Exergy efficiency (%)
PTC	17.09	79.225	23.41
TST	0.924	4.3	82.33
$Pump_1$	0.0081	0.037	25.81
$Pump_2$	0.0082	0.038	23.39
$Pump_3$	0.0009	0.004	2.425
Generator	1.116	5.2	74.08
Condenser	1.465	6.8	10.91
EV_1	0.035	0.162	84.96
Absorber	0.605	2.8	16.1
EV_2	0.0013	0.006	99.91
SHEX	0.075	0.348	73.72
Evaporator	0.243	1.126	65.96

Figure 2 illustrates the impact of generator inlet temperature (T_4) on the coefficient of performance (COP), exergy efficiency, and cooling load in a solar absorption cooling system. As T_4 increases from 170°C to 220°C, the cooling load exhibits a significant upward trend, rising from approximately 5 kW to over 10 kW, indicating that higher generator temperatures enhance the system's cooling capacity. In contrast, the COP remains nearly constant (~0.75–0.8), suggesting the system maintains efficient heat-to-cooling conversion across the temperature range. Similarly, exergy efficiency remains stable at around 0.35, implying that the exergy destruction rate is relatively unaffected by variations in T_4, even though the cooling load increases. The results indicate that increasing the generator inlet temperature does not degrade system efficiency but rather enhances cooling output, making it particularly beneficial for high-demand cooling applications in hot climates such as Tripoli, Benghazi, and Misrata. However, practical constraints such as material limitations, increased energy consumption, and potential operational costs must be considered when selecting the optimal T_4 value.

Figure 3 demonstrates how the generator inlet temperature (T_4) influences key heat transfer rates in a solar absorption cooling system, including the $\dot{Q}_{Evap}$, $\dot{Q}_{abs}$, $\dot{Q}_{cond}$, $\dot{Q}_{Gen}$, and $\dot{Q}_{SHEX}$. As T_4 increases from 170°C to 220°C, all major heat transfer rates except $\dot{Q}_{SHEX}$ show a clear upward trend. The $\dot{Q}_{Evap}$ increases significantly, indicating enhanced cooling capacity at higher generator temperatures as more refrigerants are vaporized and circulated through the system. Similarly, the absorber heat transfer rate ($\dot{Q}_{abs}$) and condenser heat transfer rate ($\dot{Q}_{cond}$) experience an increase in heat rejection, which suggests a higher refrigerant flow rate and greater cooling power but also indicates a need for effective heat dissipation to maintain system stability. The generator heat input ($\dot{Q}_{Gen}$) rises proportionally with T_4, reflecting the additional thermal energy required to separate the refrigerant from the absorbent, highlighting the trade-off between increased cooling performance and higher energy demand. Interestingly, the $\dot{Q}_{SHEX}$ remains relatively low and shows only a slight increase, indicating a stable internal heat recovery process that prevents excessive energy losses. While a higher T_4 improves system performance, it also raises the overall heat rejection in the condenser and absorber, necessitating efficient thermal management solutions such as larger heat exchangers or cooling towers.

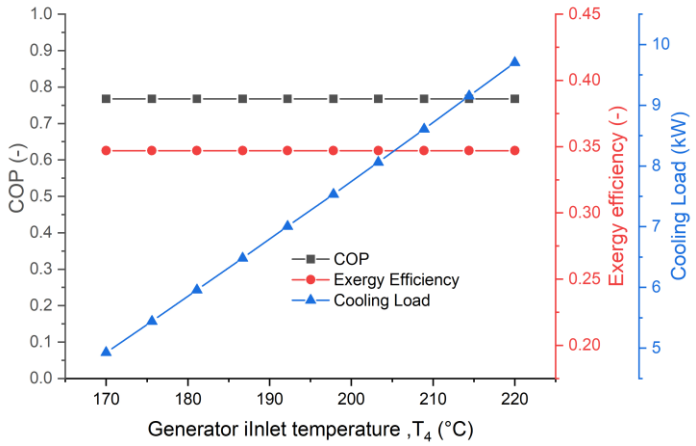

Figure 2: Effect of Generator Inlet Temperature on COP, Exergy Efficiency, and Cooling Load in a Solar Absorption Cooling System.

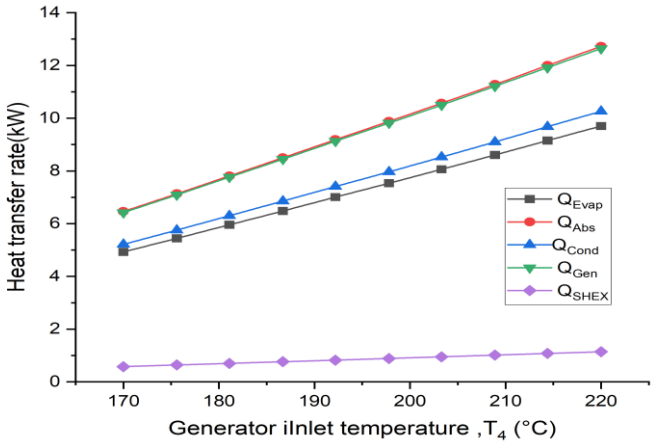

Figure 3: Effect of Generator Inlet Temperature on Heat Transfer Rates in a Solar Absorption Cooling System

Figure 4 illustrates the impact of varying evaporator temperatures (from -3°C to 6°C) on three key performance parameters in a solar absorption cooling system: COP, exergy efficiency, and cooling load. The figure reveals that COP alone is not a sufficient system performance indicator, as it remains stable while exergy efficiency declines significantly. Although the cooling load remains relatively unaffected, the exergy analysis reveals substantial performance degradation with increased evaporator temperature. COP remains nearly constant, with a very slight upward trend from around 0.74 to 0.76. A marginal increase suggests a minor improvement in thermal efficiency as the evaporator temperature increases, possibly due to a reduced temperature lift (difference between evaporator and condenser temperatures), which lowers the system's energy demand. Exergy efficiency strongly decreases with increasing evaporator temperatures from approximately 0.50 at -3°C to 0.33 at 6°C. The system experiences greater irreversibility and exergy losses at higher evaporator temperatures. Cooling load is nearly constant across the range, with a slight downward slope. It Varies slightly from 10.1 to 9.9 kW. This can be attributed to a reduced temperature gradient between the evaporator and the cooled space, decreasing the heat absorption rate.

Figure 5 illustrates how variations in evaporator temperature (ranging from -3°C to +6°C) affect heat transfer rates in five major solar absorption cooling system components. The figure shows that all heat transfer rates remain remarkably stable across the evaporator temperature ranges. The generator, absorber, condenser, and solution heat exchanger demonstrate thermal resilience and minimal sensitivity to the evaporator temperature. The slight drop in $\dot{Q}_{Evap}$ is consistent with reduced driving temperature differences as the evaporator temperature increases. $\dot{Q}_{Evap}$ is almost constant, with a very slight downward slope between 10.0 and 9.8 kW, as the heat absorbed by the evaporator decreases slightly as its temperature rises. $\dot{Q}_{Abs}$ and $\dot{Q}_{Gen}$ remain almost constant across the temperature range. Both are around 13.0 kW, as the evaporator temperature does not significantly affect these components. $\dot{Q}_{Cond}$ is also constant, around 10.8 kW. Like the absorber and generator, the condenser heat rejection is unaffected by the variation in evaporator temperature. $\dot{Q}_{SHEX}$ constant at ~1.2 kW. The solution heat exchanger remains unaffected by evaporator temperature, primarily facilitating internal energy recovery between strong and weak solutions. Its operation depends more on solution properties and generator temperature than evaporator conditions.

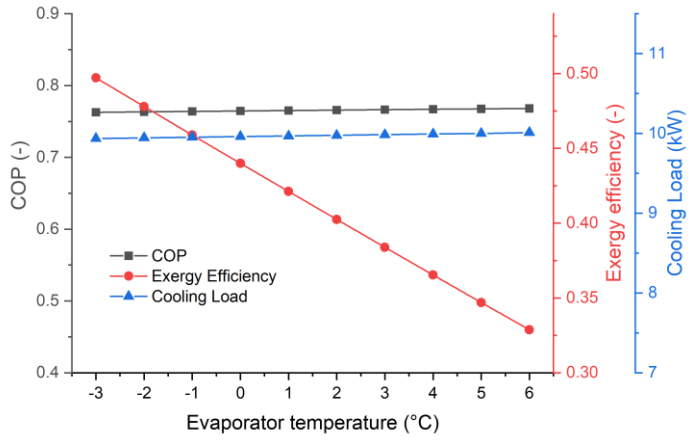

Figure 4: Effect of Evaporator Temperature on COP, Exergy Efficiency, and Cooling Load in a Solar Absorption Cooling System

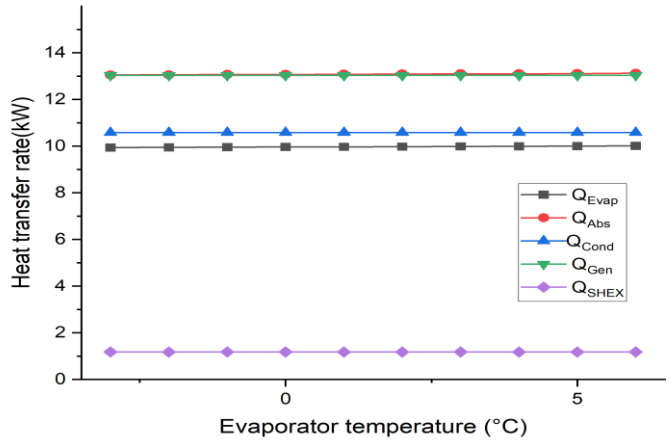

Figure 5: Effect of Evaporator Temperature on Heat Transfer Rates in a Solar Absorption Cooling System.

Figure 6 illustrates the analysis of DNI variation in Tripoli, Benghazi, and Misrata. It reveals a clear seasonal trend, with peak DNI values occurring between May and July, reaching approximately 850 W/m² in Benghazi, 830 W/m² in Tripoli and 780 W/m² in Misrata, indicating the optimal period for solar energy generation. Conversely, the lowest DNI levels are observed from November to January, dropping below 400 W/m², highlighting the need for hybrid solar systems to maintain energy supply during low-radiation months. Benghazi consistently records the highest DNI, making it the most suitable location for solar power projects, followed by Tripoli and Misrata, which receive slightly lower radiation levels due to geographical and atmospheric differences.

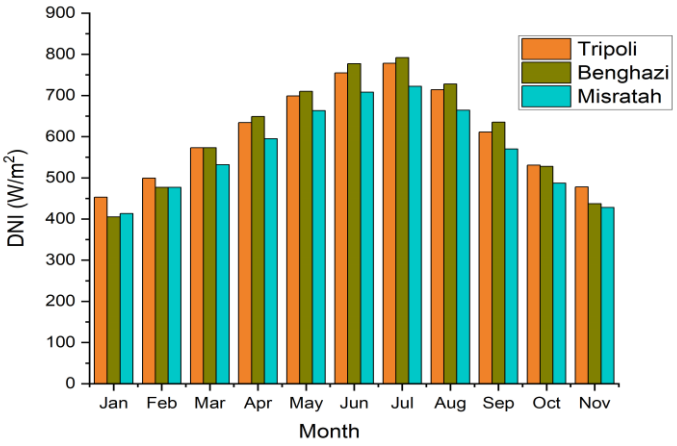

Figure 6: Monthly Variation of DNI in Tripoli, Benghazi, and Misrata

The bar chart in Figure 7 illustrates the monthly cooling load variation (kW) in Tripoli, Benghazi, and Misrata, showing a clear seasonal pattern that correlates with temperature variations and solar radiation intensity. The cooling demand gradually increases from January to June, peaking during summer (June–July) when the cooling load exceeds 10 kW in Benghazi, slightly lower in Tripoli, and the lowest in Misrata. This trend aligns with higher ambient temperatures and increased solar radiation during summer, requiring greater cooling demand to maintain indoor thermal comfort. The cooling load starts declining from August onward, reaching its lowest level between November and January (approximately 5 kW), as temperatures decrease and the need for cooling diminishes.

Benghazi consistently exhibits the highest cooling load among the three cities, likely due to higher DNI values and slightly warmer conditions than Tripoli and Misrata. Tripoli follows closely, while Misrata has the lowest cooling demand, indicating possible differences in urban heat island effects, humidity levels, and building insulation characteristics. These findings suggest that solar absorption cooling systems should be designed with higher capacities for summer months, and TES or hybrid cooling systems can help maintain efficiency during seasonal cooling variations.

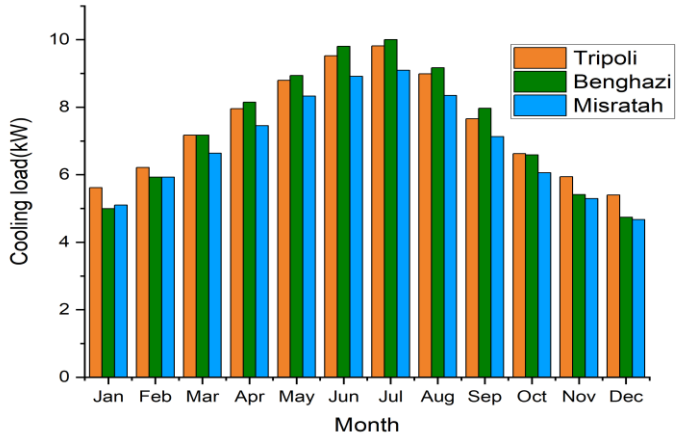

Figure 7: Monthly Variation of Cooling Load in Tripoli, Benghazi, and Misrata

Figure 8 presents the monthly solar coefficient of performance (SCOP) for three Libyan cities: Tripoli (orange), Benghazi (green), and Misrata (blue) over a full calendar year (January to December). The figure shows that SCOP values for all three cities remain within a narrow range of approximately 0.41 to 0.43 throughout the year. The highest SCOP values are observed from May to August, indicating better system efficiency during the summer months. The lowest SCOP values appear in January, February, and December, reflecting seasonal variation and reduced solar energy availability in winter. Tripoli generally shows the highest SCOP across most months. This can be attributed to its coastal location, high solar radiation, and relatively warmer temperatures throughout the year. Benghazi follows Tripoli closely and shows slightly lower SCOP values. Although also coastal, Benghazi is located further east and may receive slightly different solar profiles. Misrata consistently exhibits the lowest SCOP values of the three cities, though still within a close margin.

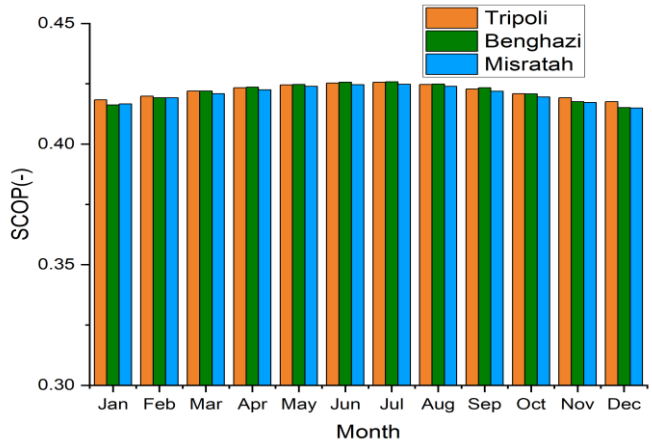

Figure 8: Monthly Variation of Solar Coefficient of Performance (SCOP) in Tripoli, Benghazi, and Misrata.

Figure 9 presents the monthly generator heat transfer rate (kW) for three Libyan cities, Tripoli, Benghazi, and Misrata, over a full calendar year (January to December). The Figure illustrates that the generator heat transfer rate varies significantly throughout the year, peaking in summer and declining in winter, in line with solar irradiance cycles. Tripoli maintains a marginal performance advantage over Benghazi and Misrata. The generator

heat transfer rate exhibits a clear seasonal pattern, increasing from January to July, peaking in July, and then decreasing until December. The lowest generator heat transfer rates were observed during the winter months (January–February) (approximately 6.5–7.5 kW) due to lower solar energy availability. A strong upward trend was observed from spring to summer (March–July); by July, rates peaked (approximately 13.5–14.2 kW). In autumn (August–December), the rate gradually decreased to winter levels, as a result of lower solar energy input. Tripoli has the highest generator heat transfer rate compared to Benghazi and Misrata in Winter (Jan–Mar and Nov–Dec). Indicates better winter solar availability or collector performance in Tripoli. Benghazi and Misrata cities show higher generator heat transfer rates than Tripoli in Summer (May–Aug). Misrata generally leads, especially in July, indicating strong summer solar input. Benghazi and Misrata benefit from better collector performance or clearer skies in the summer months.

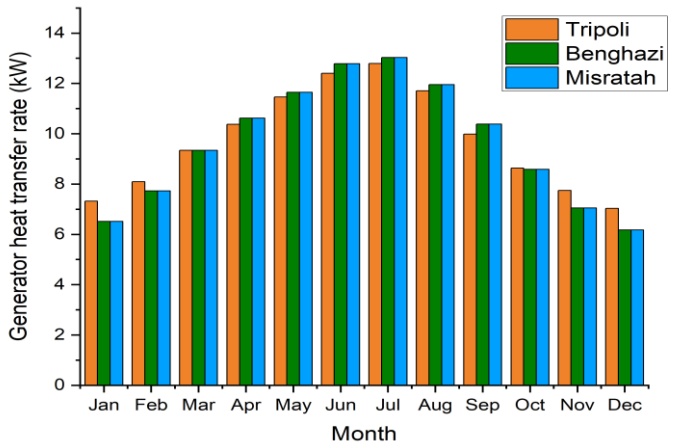

Figure 9: Monthly generator heat transfer rate (kW) in Tripoli, Benghazi, and Misrata.

4. CONCLUSION AND FUTURE WORK

This study assessed the feasibility and performance of a solar-assisted absorption cooling system tailored to the climatic conditions of Tripoli, Benghazi, and Misrata in Libya. Through energy and exergy analyses, the findings demonstrated that while the parabolic trough collector (PTC) accounts for nearly 80% of total irreversibility, other components such as the generator, solution heat exchanger, and thermal storage exhibited relatively higher efficiencies, contributing positively to overall system performance. The system achieved a stable coefficient of performance (COP) of approximately 0.75–0.8 and an exergy efficiency of about 0.35, with cooling loads surpassing 10 kW during peak summer months. These results confirm the technical viability of solar-assisted absorption systems as sustainable alternatives to conventional air conditioning in hot and arid regions.

The comparative analysis across three Libyan cities revealed important climatic dependencies: Benghazi emerged as the most suitable location due to consistently higher DNI and peak summer demand, whereas Misrata showed limitations linked to lower solar radiation and higher humidity. Tripoli, in contrast, presented balanced system behavior with moderate performance. These location-specific insights highlight the importance of adapting system design to local conditions to maximize efficiency and reliability.

Beyond technical outcomes, the research underscores the role of solar-assisted absorption cooling in addressing pressing energy security and sustainability challenges in Libya. By reducing dependence on fossil fuel-based electricity, such systems align with broader global commitments to climate change mitigation and sustainable development.

For future work, further investigations should focus on improving collector performance to reduce exergy destruction, exploring advanced multi-effect absorption configurations, and integrating hybrid systems with photovoltaic or thermal storage solutions to ensure reliability during low-solar months. Moreover, techno-economic assessments and life-cycle analyses will be essential to evaluate cost competitiveness and long-term environmental benefits, ultimately supporting wider adoption of solar-assisted cooling in Libya and similar hot-climate regions.

REFERENCESS

Akroot, A. (2025). Thermodynamic and Environmental Performance Analysis of the Marib Integrated Power and Cooling Cycle (MIPCC). *Black Sea Journal of Engineering and Science*, *8*(3), 814–823.

Akroot, A., Almaktar, M., & Alasali, F. (2024). The Integration of Renewable Energy into a Fossil Fuel Power Generation System in Oil-Producing Countries: A Case Study of an Integrated Solar Combined Cycle at the Sarir Power Plant. *Sustainability (Switzerland) , 16*(11). https://doi.org/10.3390/su16114820

Akroot, A., & Refaei, M. (2025). Thermodynamic and Exergoeconomic Assessment of a Solar-Assisted Combined Cooling, Heating, and Power System in Antalya, Turkey. *Gazi Üniversitesi Fen Bilimleri Dergisi Part C: Tasarım ve Teknoloji*, 1.

Al-Falahi, A., Alobaid, F., & Epple, B. (2020). A new design of an integrated solar absorption cooling system driven by an evacuated tube collector: A case study for Baghdad, Iraq. *Applied Sciences*, *10*(10), 3622.

Al-Falahi, A., Alobaid, F., & Epple, B. (2021). Thermo-economic comparisons of environmentally friendly solar assisted absorption air conditioning systems. *Applied Sciences*, *11*(5), 2442.

Ali, A. A. M. (2025). Annual and Decadal Temperature variability in Libya: A comprehensive Analysis (1931-2020). *The Libyan Journal of Science*, *28*(1).

Bakhshi-Jafarabadi, R., & Seyed Mousavi, S. M. (2024). Peak load shaving of air conditioning loads via rooftop grid-connected photovoltaic systems: a case study. *Sustainability*, *16*(13), 5640.

Bakouri, K., Foqha, T., Ahwidi, O., Abubaker, A., Nassar, Y., & El-Khozondar, H. (2023). Learning lessons from Murzuq-Libya meteorological station: Evaluation criteria and improvement recommendations. *Journal of Solar Energy and Sustainable Development*, *12*(1).

Bakry, K., El-Mahallawi, I., & Safwat, H. (2025). *Solar Absorption Cooling Systems–A Case Study in Egypt*.

Balghouthi, M., Chahbani, M. H., & Guizani, A. (2012). Investigation of a solar cooling installation in Tunisia. *Applied Energy*, *98*, 138–148. https://doi.org/10.1016/J.APENERGY.2012.03.017

Bindra SP, Soul F, Jabu SD, Allawafi A, Belashher AM, R. H. (2015). Potentials and Prospects of Renewables in Libya. *Prog. Clean Energy, Vol. 2 Nov*. https://doi.org/10.1007/978-3-319-17031-2_55

Birol, F. (2018). The future of cooling: opportunities for energy-efficient air conditioning. *International Energy Agency*, *526*(1).

Bodalal, A., Mashite, S., Aladouli, O., & Ihdash, A. (2017). Calculation of annual heating and cooling energy requirements for residential building in different climate zones in Libya. *Innovative Energy & Research*, *6*(2), 1463–2576.

Dawahdeh, A. I., & Al-Nimr, M. A. (2025). Energy and exergy analysis for a novel modified absorption Carnot battery. *Journal of Energy Storage*, *114*, 115779. https://doi.org/10.1016/J.EST.2025.115779

Elmorsy, L., Morosuk, T., & Tsatsaronis, G. (2020). Exergy-based analysis and optimization of an integrated solar combined-cycle power plant. *Entropy*, *22*(6), 1–20. https://doi.org/10.3390/e22060655

Elsharkawy, S. G., & Elmallah, E. S. (2016). Spatiotemporal investigation of long-term seasonal temperature variability in Libya. *Atmospheric Research*, *178*, 535–549.

Gnedi, M. D., & Robaa, S. M. (2024). Extreme climate indices over Libya: current and future outlooks. In *Hydroclimatic Extremes in the Middle East and North Africa* (pp. 343–366). Elsevier.

Hasan, A. M. A., & Mokheimer, E. M. A. (2024). Thermo-economic analysis of solar-assisted absorption systems in sun-belt cities: Saudi Arabia case studies. *Arabian Journal for Science and Engineering*, *49*(2), 2767–2795.

Hasanain, B. (2024). Fostering solar hybrid cooling systems in MENA region: A techno-economic and emission reduction assessment. *AIP Advances*, *14*(4).

Hu, T., Kwan, T. H., & Pei, G. (2022). An all-day cooling system that combines solar absorption chiller and radiative cooling. *Renewable Energy*, *186*, 831–844. https://doi.org/10.1016/J.RENENE.2022.01.058

Ibrahim, N. I., Al-Sulaiman, F. A., & Ani, F. N. (2020). A detailed parametric study of a solar driven double-effect absorption chiller under various solar radiation data. *Journal of Cleaner Production*, *251*, 119750. https://doi.org/10.1016/J.JCLEPRO.2019.119750

Imghoure, O., Belouaggadia, N., Zaite, A., Ezzine, M., Lbibb, R., & Sebaibi, N. (2024). Enhancing Energy Efficiency in Moroccan Construction through Innovative Materials: A Case Study in a Semiarid Climate. *Buildings*, *14*(10), 3087.

Lu, F., Zhu, Y., Pan, M., Li, C., Yin, J., & Huang, F. (2020). Thermodynamic, economic, and environmental analysis of new combined power and space cooling system for waste heat recovery in waste-to-energy plant. *Energy Conversion and Management*, *226*, 113511. https://doi.org/10.1016/J.ENCONMAN.2020.113511

Nourpour, M., Khoshgoftar Manesh, M. H., Pirozfar, A., & Delpisheh, M. (2023). Exergy, Exergoeconomic, Exergoenvironmental, Emergy-based Assessment and Advanced Exergy-based Analysis of an Integrated Solar Combined Cycle Power Plant. *Energy and Environment*, *34*(2), 379–406. https://doi.org/10.1177/0958305X211063558

Oye, T. T., Gupta, N., Goh, K., & Oye, T. K. (2020). Theoretical Assessment of Sustainability Principles for Renewable Smart Air-Conditioning. *Environmental Management and Sustainable Development*, *9*(3), 18–46.

Schilling, J., Hertig, E., Tramblay, Y., & Scheffran, J. (2020). Climate change vulnerability, water resources and social implications in North Africa. *Regional Environmental Change*, *20*(1), 15.

SECRETARIAT, W. (2002). Department of Economic and Social Affairs. *World*, *12*, 14.

Sivak, M. (2009). Potential energy demand for cooling in the 50 largest metropolitan areas of the world: Implications for developing countries. *Energy Policy*, *37*(4), 1382–1384. https://doi.org/10.1016/J.ENPOL.2008.11.031

Suwaed, M. S., Alturki, S. F., Ghareeb, A., Al-Rubaye, A. H., & Awad, O. I. (2023). Techno-economic feasibility of various types of solar collectors for solar water heating systems in hot and semi-arid climates: A case study. *Results in Engineering*, *20*, 101445. https://doi.org/10.1016/J.RINENG.2023.101445

Talal, W., & Akroot, A. (2023). Exergoeconomic Analysis of an Integrated Solar Combined Cycle in the Al-Qayara Power Plant in Iraq. *Processes*, *11*(3). https://doi.org/10.3390/pr11030656

Talal, W., & Akroot, A. (2024). An Exergoeconomic Evaluation of an Innovative Polygeneration System Using a Solar-Driven Rankine Cycle Integrated with the Al-Qayyara Gas Turbine Power Plant and the Absorption Refrigeration Cycle. *Machines*, *12*(2), 133. https://doi.org/10.3390/machines12020133

Tryndina, N., An, J., Varyash, I., Litvishko, O., Khomyakova, L., Barykin, S., & Kalinina, O. (2022). Renewable energy incentives on the road to sustainable development during climate change: A review. *Frontiers in Environmental Science*, *10*, 1016803.

Wang, J., Lu, Z., Li, M., Lior, N., & Li, W. (2019). Energy, exergy, exergoeconomic and environmental (4E) analysis of a distributed generation solar-assisted CCHP (combined cooling, heating and power) gas turbine system. *Energy*, *175*, 1246–1258. https://doi.org/10.1016/j.energy.2019.03.147

Weltbankgruppe. (2021). *The cold road to Paris: mapping pathways toward sustainable cooling for resilient people and economies by 2050*. World Bank.